



# Origin of Great Unconformity Obscured by Thermochronometric Uncertainty

Matthew Fox<sup>1</sup>, Adam G.G Smith<sup>1</sup>, Pieter Vermeesch<sup>1</sup>, Kerry Gallagher<sup>2</sup>, Andrew Carter<sup>3</sup>

<sup>1</sup> London Geochronology Centre, Department of Earth Sciences, University College London, Gower St., London, WC16BT, UK

<sup>2</sup> Géosciences Rennes/OSUR, University of Rennes, Rennes, France

<sup>3</sup> London Geochronology Centre, Department of Earth Sciences, Birkbeck College, Gower St., London, WC16BT, UK

Correspondence to: Matthew Fox ([m.fox@ucl.ac.uk](mailto:m.fox@ucl.ac.uk))

**Abstract.** Thermochronology provides a unique perspective on the magnitude of rock that is eroded during, and the timing of, unconformities in the rock record. Recently, thermochronology has been used to reinvigorate a long-standing debate about the origin of the Great Unconformity, a global erosional event that represents a time period of almost a billion years at the end of the Precambrian. The (U-Th)/He in zircon system is particularly well suited to provide this perspective because it is very sensitive to long durations of time at relatively low temperatures (< 200-250°C). However, the diffusion kinetics of <sup>4</sup>He in zircon change dramatically as a result of radiation damage to the crystal lattice. Therefore, our ability to resolve thermal histories is fundamentally limited by how well we know parameters controlling helium diffusion and their uncertainties. Currently, there is no estimate of how these uncertainties impact the inferred thermal histories. Here we determine uncertainties in the Zircon Radiation Damage and Annealing Model (ZRDAAM, Guenther et al. 2013) that describes changes in <sup>4</sup>He diffusion kinetics as a function of radiation damage. We show that the dispersion in predicted zircon (U-Th)/He ages for a given thermal history can be 100s Ma for a specific amount of radiation damage and that thermal histories are less well resolved than previously appreciated. Additional diffusion experiments and calibration with natural laboratories would provide better constraints on diffusion kinetic parameters.

## 1. Introduction

Thermochronometry is widely used to constrain the evolution of Earth's surface and upper crust, transforming our understanding of the magnitudes of sedimentation and erosion linked to climate and tectonic change. Notably, thermochronometry has been used recently to understand the development of



the Great Unconformity (DeLucia et al., 2018; Keller et al., 2019; Flowers et al., 2020; McDannell et al., 2022), a global feature that marks the boundary between the Precambrian and Phanerozoic. The time-period that the Great Unconformity spans varies depending on location, but on the North American craton, in the Grand Canyon, the erosional event spans from circa 1200 to 250 million years (Thurston et al., 2022). The origin of the Great Unconformity has been debated for over 125 years, with recent contributions using thermochronometry to gain new insight (McDannell et al., 2022). This approach highlighted that erosion rates increased across the North American craton during Neoproterozoic glaciation, supporting the hypothesis that the Great Unconformity is the result of glacial erosion (Keller et al., 2019), as opposed to diachronous tectonic events (Flowers et al., 2020).

The principle behind thermochronometry is that rocks experience temperature changes over geological timescales: rocks closer to Earth's surface are cooler than deeper ones and so exhumation leads to cooling. The time scales associated with these changes in temperature are determined using the concepts of geochronology. The daughter products of radioactive decay used for thermochronometry have a temperature dependent rate of loss from the target mineral. At high temperatures the daughter products are effectively lost instantaneously. By contrast, as the rock cools to lower temperatures, the rate of diffusive decreases and daughter products are progressively retained until there is effectively no diffusive loss. Therefore a measured age reflects the duration of residence at low temperature (Dodson, 1973; Zeitler et al., 1987; Reiners, 2005).

One of the most widely used methods for deep-time thermochronometry is (U-Th)/He in zircon (ZHe) (Reiners, 2005). The basis of this method is that the radioactive elements uranium and thorium are incorporated into crystals of zircon and the decay product, helium, is trapped in the crystal lattice. Helium diffuses from zircon at high temperatures, but is retained at lower temperatures. The exact temperature range at which the transition from closed-system to open-system behaviour occurs is dependent on damage to the crystal lattice produced primarily from recoil during decay processes (Guenther et al., 2013). Radiation damage accumulates at a rate that depends on the amount of uranium, thorium, and samarium in the crystal. This means that two zircon crystals from the same rock, experiencing the same thermal history, could have very different thermal sensitivity. In turn, models accounting for this variable temperature sensitivity as a function of radiation damage can be used to leverage more complex thermal histories than constant kinetic parameter models. This approach has successfully been used to infer deep-time erosion rate histories, and in the case of the Great



65 Unconformity, has reinvigorated debate on its origin (Flowers et al., 2020; Peak et al., 2021;  
 McDannell et al., 2022)

Both those in favour of a glacial (McDannell et al., 2022) and tectonic (Flowers et al., 2020) origin of  
 the Great Unconformity have interpreted ZHe data using the Zircon Radiation Damage And Annealing  
 Model (ZRDAAM) of Guenther et al. (2013). In this model, a crystal is composed of undamaged and  
 70 damaged parts that combine to give bulk diffusion kinetics as a function of the amount of radiation  
 damage. Accumulated radiation damage is calculated based on the concentrations of the parent  
 elements and the thermal history of a sample. The damage accumulates at low temperatures, but can be  
 annealed at higher temperatures, calculated using fission track annealing kinetics (Yamada et al., 1995;  
 Rahn et al., 2004; Tagami, 2005; Yamada et al., 2007). Therefore, the diffusivity of helium at a specific  
 75 temperature is a function of the past thermal history. This makes the overall problem very non-linear so  
 that changing the temperature at some time in the thermal history can have unexpected effects on the  
 resulting age, as also shown for the (U-Th)/He in apatite system by Fox and Shuster (2014).

Using the radiation damage and annealing model (RDAAM) with inverse models, researchers have  
 80 resolved tight temperature constraints on thermal histories over billion year timescales. For example,  
 Thurston et al. (2022) inferred a 1700 Ma thermal history from ZHe ages in Eastern Grand Canyon.  
 Parts of this history were reported to within less than 10 degrees between 700 and 250 Ma and then  
 again from 15 -7 Ma. It is unclear whether the data really provide such tight constraints on  
 temperatures in the past or whether these are at least partly the consequence of model assumptions  
 85 and/or, potentially, overconfidence in the adopted diffusion kinetic parameters.

Calibration of ZRDAAM has been carried out using measured diffusion kinetics of crystals with known  
 amounts of radiation damage (Guenther et al., 2013). However, the accuracy and precision of this  
 model has not been assessed. In particular, it is unclear how the propagation of uncertainties to model  
 90 parameters affects the dispersion or sensitivity of predicted thermochronometric ages. Here we show  
 that the uncertainties in the radiation damage model make it challenging to accurately infer the timing  
 and magnitude of unconformities in the deep past. We begin by highlighting why ZRDAAM needs to  
 be calibrated accounting for uncertainties and present our new calibration. We then propagate  
 uncertainties from this model calibration through time temperature paths. We show that natural  
 95 variability in radiation damage annealing parameters causes ZHe ages to be very dispersed even for  
 crystals of the same size and radiation damage levels. Using QTQt (Gallagher, 2012), we show that



different diffusion kinetics can lead to the onset of cooling for resolved thermal histories from inverse methods varying by hundreds of millions of years.

## 100 2. The existing calibration of the radiation damage and annealing model

The rate of diffusion is controlled by the diffusivity and the curvature of the concentration of the diffusant (Fick's Law). Although the production distribution of the diffusant (helium in our case) can be important in some scenarios, diffusion tends to smooth the distribution. More significant is the fact that the diffusivity can vary by orders of magnitude with variations in temperature. The diffusivity at  
 105 any temperature is given by the Arrhenius equation of the diffusivity  $D$  ( $\text{cm}^2/\text{s}$ ):

$$D(T) = D_0 e^{\frac{-E_a}{RT}} \quad (1)$$

where  $D_0$  is the frequency factor ( $\text{cm}^2/\text{s}$ ),  $E_a$  is the activation energy ( $\text{kJ/mol}$ ),  $R$  is the gas constant  
 110 ( $\text{J/K/mol}$ ) and  $T$  is the temperature in Kelvin. Taking the logarithm of equation 1, gives:

$$\ln(D(T)) = \frac{-E_a}{R} \frac{1}{T} + \ln(D_0) \quad (2)$$

so that the slope of the line between  $\ln(D(T))$  and  $1/T$  gives  $E_a/R$  and the intercept of the line provides  
 115  $\ln(D_0)$ . Diffusion experiments in which a crystal is step-wise degassed *in vacuo* are used to calculate  
 $D(T)$  for different combinations of specific temperatures and time (Fechtig and Kalbitzer, 1966). The  
 resulting plot can be used to determine the Arrhenius parameters ( $D_0$ ,  $E_a$ ). Importantly, estimates of the  
 two model parameters extracted from this linear inversion covary with one another, i.e.,  $\ln(D_0)$  is  
 strongly correlated with  $E_a$ .

120 Analyzing different crystals with known radiation damage values allows us to assess how diffusion  
 kinetics vary with damage. It is challenging to visualize both model parameters ( $D_0$  and  $E_a$ ) for each  
 crystal as a function of radiation damage and so it is common to combine the parameters and calculate  
 a diffusivity at a specific temperature or a closure temperature at a specific cooling rate. By combining  
 the parameters, however, information on how the two parameters are correlated is lost.

125

The results of Guenther et al., (2013)'s diffusion experiments highlight two general trends. At low  
 damage values the closure temperature increases with increasing damage. At higher damage values, the  
 closure temperature decreases with increasing damage. This general behaviour has been reproduced in



numerical models conducted at a range of scales (Ketcham et al., 2013; Gautheron et al., 2020). To  
 130 interpret these trends in ZRDAAM, a model is used in which the diffusion kinetics for a specific  
 radiation damage value are a combination of a theoretical minimally damaged crystal and an extremely  
 damaged crystal. The diffusion kinetics of these end-member crystals need to be estimated. The  
 frequency factor of the minimally damaged crystal ( $^{\circ}D_0$ ) was estimated by extrapolating the frequency  
 factors of measured crystals down two orders of magnitudes using a power-law relationship. The  
 135 activation energy for theoretical crystal ( $^{\circ}E_a$ ) is set as the average of the activation energies of  
 minimally damaged crystals (see Guenthner et al., 2013 for details). Extrapolating values to a  
 minimally damaged crystal, however, will add uncertainties and there is no obvious way to account for  
 these in the power-law relationship. Crucially, this approach does not account for the correlations  
 between the model parameters. This is important because the correlations provide additional  
 140 information that can yield more precise estimates of model parameters and allow propagation of  
 uncertainties into model predictions. The diffusion kinetics for the extremely damaged crystal are  
 estimated using sample N17 (Guenthner et al., 2013), and also involve correlated model parameters  
 ( $^{N17}D_0$  and  $^{N17}E_a$ ). However, the accuracy of this model has only been assessed by looking at general  
 trends in model predictions. Here we attempt to formally quantify the uncertainty in model parameters  
 145 and how these uncertainties translate to uncertainties in temperature sensitivity of the ZHe system, and  
 in particular predicted ZHe ages.

### 3. A new calibration of the zircon radiation damage and annealing model

150 In order to account for the correlation between the frequency factor and the activation energy, we  
 model the measured helium diffusivities directly. We use the same diffusion data and parameterisation  
 as Guenthner et al. (2013). However, in contrast with Guenthner et al. (2013), we determine the  
 diffusion of the end member crystals using the radiation damage model directly, rather than by non-  
 linear extrapolation from high to low radiation damage levels. Our goal is not to simply increase the  
 155 accuracy of the model parameters but to determine their precision. By tracking correlations in model  
 parameters, we can simulate (U-Th)/He in zircon ages accounting for uncertainties in the original  
 diffusion experiments.

The model we fit is given by equation 8 of Guenthner et al. (2013) and describes the diffusivity  $D$  as a  
 160 function of the amount of damage:



$$\frac{1}{\frac{D}{a^2}} = \frac{f'_c}{\frac{1}{\left(\frac{l_{int,0}}{l_{int}}\right)^2} * \left(\frac{D_z}{(a * f'_c)}\right)} + \frac{f'_a}{\frac{D_{N17}}{(a * f'_a)^2}}$$

(4)

165 where  $f'_c$  and  $f'_a$  are the crystalline and amorphous fractions, respectively,  $l_{int}$  and  $l_{int,0}$  are parameters  
 describing how far a helium atom can travel within a crystal lattice without encountering damage in a  
 damaged crystal and an undamaged crystal respectively, and  $a$  is the grain size.  $D_z$  and  $D_{N17}$  can be  
 calculated using the diffusion kinetics of the undamaged and damaged theoretical crystals, using  
 equation 4. Therefore, for every sample with a known amount of damage, we can calculate different  
 170 diffusivity values for degassing steps using model parameters  $^{N17}D_0$  and  $^{N17}E_a$  for  $D_{N17}$  and  $^zD_0$  and  $^zE_a$   
 for  $D_z$ . We use the Bayesian Markov Chain Monte Carlo (MCMC) method incorporating the  
 Metropolis-Hastings algorithm to sample the full posterior distribution of the model parameters. We  
 tune the proposal distributions to ensure that approximately 20% of the proposed models are accepted  
 as this represents an efficient balance between exploring parameter space and sampling the parameter  
 175 values. The Markov Chain is initialised with the model parameters of Guenther et al. (2013) and the  
 algorithm runs until 1 million sets of model parameters have been accepted. The likelihood function is  
 defined as a least squares fit to the data. However, the degassing experiments of Guenther et al. (2013)  
 each have different numbers of steps. The likelihood function involves a summation, related to the  
 number of steps, and so number of data points in each experiment, experiments with more steps would  
 180 tend to dominate our results. Similarly, key experiments which might have fewer steps would have far  
 less influence on the model parameter estimation. To account for this problem, the misfit for each  
 experiment is weighted accordingly, so that the log-likelihood (LL) function is:

$$LL = 0.5 * \sum_{i=1}^N \frac{1}{M_i} \sum_{j=1}^{M_i} \left( \frac{D_{i,j} - P_{i,j}}{\sigma} \right)^2$$

(5)

185 where  $N$  is the number of crystals analyzed,  $M_i$  is the number of degassing steps used in the inversion  
 for a specific crystal,  $D_{i,j}$  is the observed diffusivity for a specific crystal at a specific degassing step,  $P_{i,j}$   
 is corresponding predicted diffusivity calculated with Equation 4, and  $\sigma$  is the estimated uncertainty  
 set to  $1 \ln(1/s)$  here, based on reported uncertainties. Preliminary experiments highlighted that the  
 190 sampling was relatively insensitive to the diffusion kinetics of the damaged N17 crystal. To ensure that



the diffusion kinetics of this unique and crucial end member crystal was accurately captured, we reduced the uncertainty of the diffusion data for N17 to  $0.1 \ln(1/s)$ .

The comparison of the predicted and observed diffusivities for the best fitting model is shown in Figure 1B. We also show the model fit with the original Guenther et al., (2013) parameters in Figure 1A. Results of our analysis are plotted as 4 histograms showing the original model parameters and our inferred model parameters (Figure 2). The posterior probability of the model parameters is proportional to the height of the model histograms. For the amorphous crystal, our maximum a posteriori model parameter values are close to the original values, shown in red. However, for the low-damaged crystal, the model predictions are quite different, although we note that the original values are close to the 2D probability peak (Figure 3) which accounts for model correlations. Additionally, we will focus on the overall spread in the values of these model parameters and we explore the importance of this variability in the next section.

#### 4. Propagating model uncertainties

To assess the importance of the uncertainties in the radiation damage and annealing model parameters, we predict ages using a simple thermal model. The time-temperature path is chosen to resemble that of the Minnesota samples from McDannell et al. (2022), and represents a typical inferred time temperature path of a Deep Time target locality. Here the rocks have been below  $600^{\circ}\text{C}$  since 1.5 Ga. From 700 Ma to 650 Ma the rocks cooled from  $200$  to  $150^{\circ}\text{C}$ , and then gradually to  $0^{\circ}\text{C}$  by 200 Ma before experiencing reheating at 50 Ma to  $100^{\circ}\text{C}$ . Between 50 Ma and the present the rocks cooled linearly to  $0^{\circ}\text{C}$ . Radiation damage accumulates throughout this history such that some zircon crystals that transitioned from open to closed system behaviour during the cooling event at 700 Ma, transitioned back to open behaviour simply due to the accumulation of radiation damage. Some crystals however, with intermediate temperature sensitivity only record the final cooling event. Other crystals, with low-temperature sensitivity, also record cooling associated with the 100 Ma burial event. In terms of constraining thermal history models, this potential to have a wide range of temperature sensitivities within a single sample makes the ZHe method very powerful.

To calculate thermochronometric ages we use the radiation damage and annealing model of Guenther et al. (2013) with our updated model parameters. Note, this implementation of the model has been used previously (Tripathy-Lang et al., 2015). 20 different crystals are simulated spanning an effective U



concentration ( $[eU] = [U] + 0.24[Th]$ ; Gastil et al., (1967)) interval from 31 to 2828 ppm. Ages for these  
 225 20 different crystals are calculated 200 times with different model parameters for  $^{17}D_0$ ,  $^{17}E_a$ ,  $^{17}D_0$  and  
 $^{17}E_a$ . To do this, we extracted every 100<sup>th</sup> model from the posterior ensemble of models generated  
 during the MCMC algorithm. This ensures that we are sampling model parameter space in proportion  
 to probability but also that the model correlations are reliably captured. Grain sizes are all set to 70  $\mu m$ .  
 230 The results highlight the large spread in predicted ages for a single thermal history (Figure 4). The  
 overall spread in age is expected given the different temperature sensitivity of the crystals. However,  
 even for a specific amount of radiation damage there is still a large dispersion in the predicted ages. For  
 example, at  $[eU]$  values of about 1600 ppm, ages are expected to vary between 50 and 550 Ma. If a  
 range of grain sizes were also modelled for a specific  $[eU]$ , the spread would be even larger.  
 235 Furthermore, a myriad of other factors will also contribute to this dispersion (see Fox et al., 2019 for a  
 discussion).

In order to highlight how uncertainty in diffusion parameters propagate to uncertainty in thermal  
 histories, we use QTQt (Gallagher 2012) and the data from McDannell et al. (2022). It is important to  
 240 note that our goal is not to determine a new thermal history from the data, but rather to assess  
 uncertainties related to the kinetics. For this reason, we only use only the ZHe data and do not  
 incorporate additional constraints. We use the 22 ZHe single grain age data for the sample “Minnesota”  
 of McDannell et al. (2022), and 2 sets of values for the 4 diffusion parameters based on the MCMC  
 sampling. These correspond to values of 129224.284308, 4.000427, 149756.087043, 4.130064 and  
 245 42388.297312, -5.000653 137904.535009, 3.253373 corresponding to  $^{17}E_a$ ,  $\log_{10}(^{17}D_0)$ ,  $^{17}E_a$  and  
 $\log_{10}(^{17}D_0)$  for a high value for the frequency factor of N17 and a low value, respectively. We also use  
 the values originally proposed by Guenthner et al. (2013) as a reference. The priors for time and  
 temperature were specified to be  $1500 \pm 1500$  M.y. and  $150 \pm 150^\circ C$  respectively. We ran the sampler for  
 300k iterations burn-in and 300k post-burn-in, accepting models in the conventional MCMC way, such  
 250 that a proposed model of equal likelihood to the current model will be accepted irrespective of the  
 complexity. Results show that while the general trend of the cooling is very similar, the posterior  
 probabilities are all quite different (Figure 5). This has important implications for our ability to reliably  
 identify cooling signatures. In particular, the part of the thermal history that appears well resolved by  
 the data changes from 1000 Ma to 1500 Ma depending on the choice of radiation damage parameters.  
 255 This suggests that the resolution in estimating the timing of a given cooling event could be as large as  
 500 Ma, with obvious implications for resolving the timing of the Great Unconformity.





## 5. Implications

260 Our method to propagate ZRDAAM uncertainty highlights how variable the age-[eU] relationship  
 might be for a given thermal history. In particular, our results suggest that the uncertainty of  
 ZRDAAM-based thermal history inversions may be significantly underestimated. This has major  
 implications for our ability to differentiate between subtle differences in temperature at specific times.  
 In turn, it may be challenging to resolve cooling histories sufficiently to attribute the Great  
 265 Unconformity to Cryogenic Glaciations (McDannell et al., 2022) or geodynamic processes related to  
 the break-up of Gondwana (Flowers et al., 2020).

The potential to underestimate age uncertainty for thermal modelling has been discussed by McDannell  
 et al. (2022) and to some extent this can be accounted for in the inverse modelling software QTQt  
 270 (Gallagher, 2012). For example, if two dates have the same [eU] but their measured uncertainties do  
 not overlap, QTQt can sample additional uncertainty for the measurements to account for this excess  
 dispersion. However, if the two ages do not have the same [eU] concentration, the situation is more  
 difficult. Either additional uncertainty can be assigned to the measurements by resampling a scaling  
 factor ( $> 1$ ) that multiplies the input errors. This tends to allow the predicted age-[eU] relationship to  
 275 pass through the observed data+resampled uncertainty. Or, alternatively, the thermal history can be  
 adjusted to change the predicted age-[eU] relationship to try and ensure that the predictions fit the data,  
 at least to within the error. The first option tends to produce simpler thermal histories than the second  
 option, as the data fitting criterion is less strict. For example, McDannell et al. (2022)'s results for  
 Pikes Peak highlight how models that ignore overdispersion appear to resolve a 700 Ma cooling  
 280 signature, which is smoothed out when the overdispersion is effectively reduced by adding excess  
 uncertainty on some of the data.

We have shown the continuous spread of ages as a function of [eU] as a probability heat map for a  
 specific history (Figure 4). In reality, most thermochronometric studies analyse 5-30 crystals for each  
 285 sample. We can illustrate the effect of model uncertainty by comparing two simulated datasets of 15  
 ages generated from the same thermal history. We can produce these datasets by sampling our age  
 probability distribution randomly (Figure 6). Although these two datasets display overall similarities,  
 there are subtle differences between their age-[eU] relationship over specific [eU] values. To accurately  
 capture the spread in age for a single radiation damage value, many more thermochronometric samples



290 would need to be collected. To illustrate this point, we draw random samples from the probability  
 distribution in figure 4, for [eU] values ranging from 1500 to 2000 ppm, and investigate the spread in  
 age (Figure 6). The dispersion of the ages varies greatly with increasing sample size, converging to the  
 predicted frequency distribution of figure 4. In our specific example, the distribution stabilises for  
 sample sizes of 40 crystals. The need to accurately capture spread are especially important if ages need  
 295 to be averaged within [eU] bins to find acceptable paths as the uncertainty for the mean age is  
 determined by the standard deviation (Flowers et al., 2020; Peak et al., 2021; Thurston et al., 2022).  
 Ault et al. (2018) showed that simple visual identification under the microscope of the degree of  
 metamictization is useful for obtaining good [eU] coverage and this approach could be adopted to  
 ensure that multiple ages for the same [eU] are measured to get an idea of the spread in age.

300

The large uncertainties on the parameters controlling helium diffusion in zircon and the dramatic  
 impact this has on temperature sensitivity highlights that this is important to consider. Currently, it is  
 not practical to incorporate diffusion kinetic uncertainties in inverse models directly because this  
 dramatically increases the volume of the parameter space that needs to be searched and would lead to  
 305 long run times. However, with the development of faster computers and parallelized inverse methods,  
 this may be possible. Crucially, to ensure that we sample crystals with the same [eU] values to resolve  
 diffusion kinetic parameters, many more ages per sample need to be analysed. For example, to  
 accurately capture the spread in age for a relatively narrow [eU] range of 1500-2000 ppm, 40 crystals  
 from this interval were required (Figure 6). A practical solution to avoid measuring so many crystals  
 310 per sample and running millions of simulations in an inversion is to use forward modelling. To do this,  
 a single thermal history that is close to what might be expected for a specific area given prior  
 knowledge could be used to assess expected age spread. This expected age spread could then be added  
 to the age uncertainties used for inverse modelling. This procedure could be iterated to produce realistic  
 uncertainties.

315

ZRDAAM has been calibrated using a limited number of diffusion experiments. Additional work is  
 required to develop this dataset to capture diffusion kinetics at different radiation damage values. These  
 experiments could also aim to replicate diffusion kinetics at previously measured radiation damage  
 values to quantify the degree of dispersion. In addition, natural laboratories could be utilised to resolve  
 320 diffusion parameters: areas with known thermal histories can be exploited to predict ZHe ages by  
 varying diffusion parameters; complementary thermochronometers can be leveraged to find thermal  
 histories and diffusion parameters that match the observed data. Ultimately, by reducing the



uncertainties in helium diffusion kinetics using the constraints from man-made and natural laboratories,  
 the timings of cooling events in the past can be resolved with more accuracy and precision.

325

**Code availability.** Codes required for this analysis can be requested from the authors.

**Data availability.** No new data were generated for this analysis.

**Author contributions.** MF designed the analysis, carried out the uncertainty modelling. AS, PV and  
 AC contributed to the concepts discussed. KG carried out the QTQt modelling. All authors contributed  
 to writing.

330

**Competing interests.** The authors declare no competing interests.

#### Acknowledgements

We thank W. Guenther for sharing data used for the calibration and for comments on an earlier  
 version of the manuscript. This study was supported by NERC (NE/N015479/1).

335

#### References

Ault, A.K., Guenther, W.R., Moser, A.C., Miller, G.H. and Refsnider, K.A.: Zircon grain selection  
 reveals (de) coupled metamictization, radiation damage, and He diffusivity. *Chemical Geology*, 490, 1-  
 12, <https://doi.org/10.1016/j.chemgeo.2018.04.023>, 2018

340

DeLucia, M. S., Guenther, W. R., Marshak, S., Thomson, S. N., and Ault, A. K.: Thermochronology  
 links denudation of the Great Unconformity surface to the supercontinent cycle and snowball Earth,  
*Geology*, 46, 167–170, <https://doi.org/10.1130/G39525.1>, 2018.

345

Dodson, M. H.: Closure temperature in cooling geochronological and petrological systems, *Contrib.*  
*Mineral. Petrol.*, 40, 259–274, <https://doi.org/10.1007/BF00373790>, 1973.

Fechtig, H. and Kalbitzer, S.: The Diffusion of Argon in Potassium-Bearing Solids, in: *Potassium*  
*Argon Dating*, Springer Berlin Heidelberg, Berlin, Heidelberg, 68–107, [https://doi.org/10.1007/978-3-642-87895-4\\_4](https://doi.org/10.1007/978-3-642-87895-4_4), 1966.

350

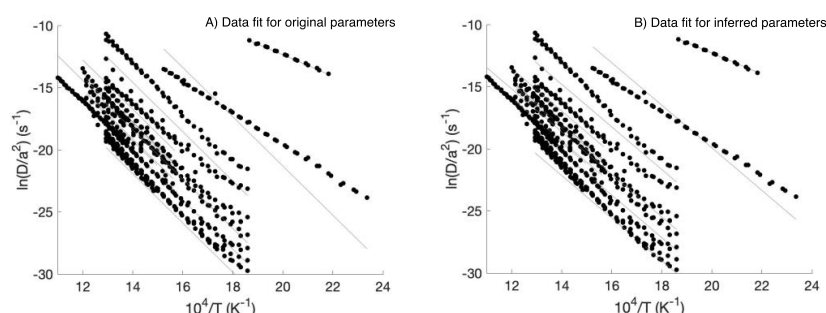
Flowers, R. M., Macdonald, F. A., Siddoway, C. S., and Havranek, R.: Diachronous development of  
 Great Unconformities before Neoproterozoic Snowball Earth, *Proc. Natl. Acad. Sci.*, 117, 10172–  
 10180, <https://doi.org/10.1073/pnas.1913131117>, 2020.



- 355 Fox, M. and Shuster, D. L.: The influence of burial heating on the (U–Th)/He system in apatite: Grand Canyon case study, *Earth Planet. Sci. Lett.*, 397, 174–183, <https://doi.org/10.1016/j.epsl.2014.04.041>, 2014.
- Fox, M., Dai, J., and Carter, A.: Badly Behaved Detrital (U–Th)/He Ages: Problems With He Diffusion Models or Geological Models?, *Geochem. Geophys. Geosystems*, 2018GC008102, <https://doi.org/10.1029/2018GC008102>, 2019.
- 360 Gallagher, K.: Transdimensional inverse thermal history modeling for quantitative thermochronology, *J. Geophys. Res. Solid Earth*, 117, n/a–n/a, <https://doi.org/10.1029/2011JB008825>, 2012.
- Gautheron, C., Djimbi, D.M., Roques, J., Balout, H., Ketcham, R.A., Simoni, E., Pik, R., Seydoux-Guillaume, A.M. and Tassan-Got, L.: A multi-method, multi-scale theoretical study of He and Ne diffusion in zircon. *Geochimica et Cosmochimica Acta*, 268, pp.348–367. <https://doi.org/10.1016/j.gca.2019.10.007>, 2020
- 365 Gordon Gastil, R., DeLisle, M., and Morgan, J.: Some Effects of Progressive Metamorphism on Zircons, *Geol. Soc. Am. Bull.*, 78, 879, [https://doi.org/10.1130/0016-7606\(1967\)78\[879:SEOPMO\]2.0.CO;2](https://doi.org/10.1130/0016-7606(1967)78[879:SEOPMO]2.0.CO;2), 1967.
- 370 Guenther, W. R., Reiners, P. W., Ketcham, R. A., Nasdala, L., and Giester, G.: Helium diffusion in natural zircon: Radiation damage, anisotropy, and the interpretation of zircon (U–Th)/He thermochronology, *Am. J. Sci.*, 313, 145–198, <https://doi.org/10.2475/03.2013.01>, 2013.
- Keller, C. B., Husson, J. M., Mitchell, R. N., Bottke, W. F., Gernon, T. M., Boehnke, P., Bell, E. A., Swanson-Hysell, N. L., and Peters, S. E.: Neoproterozoic glacial origin of the Great Unconformity, *Proc. Natl. Acad. Sci.*, 116, 1136–1145, <https://doi.org/10.1073/pnas.1804350116>, 2019.
- 375 Ketcham, R.A., Guenther, W.R. and Reiners, P.W.: Geometric analysis of radiation damage connectivity in zircon, and its implications for helium diffusion. *American Mineralogist*, 98(2–3), pp.350–360. <https://doi.org/10.2138/am.2013.4249>, 2013
- McDannell, K. T., Keller, C. B., Guenther, W. R., Zeitler, P. K., and Shuster, D. L.: Thermochronologic constraints on the origin of the Great Unconformity, *Proc. Natl. Acad. Sci.*, 119, e2118682119, <https://doi.org/10.1073/pnas.2118682119>, 2022.



- 380 Peak, B. A., Flowers, R. M., Macdonald, F. A., and Cottle, J. M.: Zircon (U-Th)/He thermochronology reveals pre-Great Unconformity paleotopography in the Grand Canyon region, USA, *Geology*, 49, 1462–1466, <https://doi.org/10.1130/G49116.1>, 2021.
- Rahn, M. K., Brandon, M. T., Batt, G. E., and Garver, J. I.: A zero-damage model for fission-track annealing in zircon, *Am. Mineral.*, 89, 473–484, <https://doi.org/10.2138/am-2004-0401>, 2004.
- 385 Reiners, P. W.: Zircon (U-Th)/He Thermochronometry, *Rev. Mineral. Geochem.*, 58, 151–179, <https://doi.org/10.2138/rmg.2005.58.6>, 2005.
- Tagami, T.: Zircon Fission-Track Thermochronology and Applications to Fault Studies, *Rev. Mineral. Geochem.*, 58, 95–122, <https://doi.org/10.2138/rmg.2005.58.4>, 2005.
- Thurston, O. G., Guenther, W. R., Karlstrom, K. E., Ricketts, J. W., Heizler, M. T., and Timmons, J.
- 390 M.: Zircon (U-Th)/He thermochronology of Grand Canyon resolves 1250 Ma unroofing at the Great Unconformity and <20 Ma canyon carving, *Geology*, 50, 222–226, <https://doi.org/10.1130/G48699.1>, 2022.
- Tripathy-Lang, A., Fox, M., and Shuster, D. L.: Zircon 4He/3He thermochronometry, *Geochim. Cosmochim. Acta*, 166, 1–14, <https://doi.org/10.1016/j.gca.2015.05.027>, 2015.
- 395 Yamada, R., Tagami, T., Nishimura, S., and Ito, H.: Annealing kinetics of fission tracks in zircon: an experimental study, *Chem. Geol.*, 122, 249–258, [https://doi.org/10.1016/0009-2541\(95\)00006-8](https://doi.org/10.1016/0009-2541(95)00006-8), 1995.
- Yamada, R., Murakami, M., and Tagami, T.: Statistical modelling of annealing kinetics of fission tracks in zircon; Reassessment of laboratory experiments, *Chem. Geol.*, 236, 75–91, <https://doi.org/10.1016/j.chemgeo.2006.09.002>, 2007.
- 400 Zeitler, P. K., Herczeg, A. L., McDougall, I., and Honda, M.: U-Th-He dating of apatite: A potential thermochronometer, *Geochim. Cosmochim. Acta*, 51, 2865–2868, [https://doi.org/10.1016/0016-7037\(87\)90164-5](https://doi.org/10.1016/0016-7037(87)90164-5), 1987.



405

**Figure 1.** Key parameters controlling how radiation damage controls diffusivity have been inferred from fitting Arrhenius relationships from step-degassing experiments. A) The fit to the step-degassing experiments for the model parameters inferred by Guenther et al., (2013). B) The fit to the step-degassing experiments using model parameters extracted from the data using a Markov Chain Monte Carlo analysis. The model parameters are the minimum misfit model parameters and represent a single realization of the parameter set we infer.

415

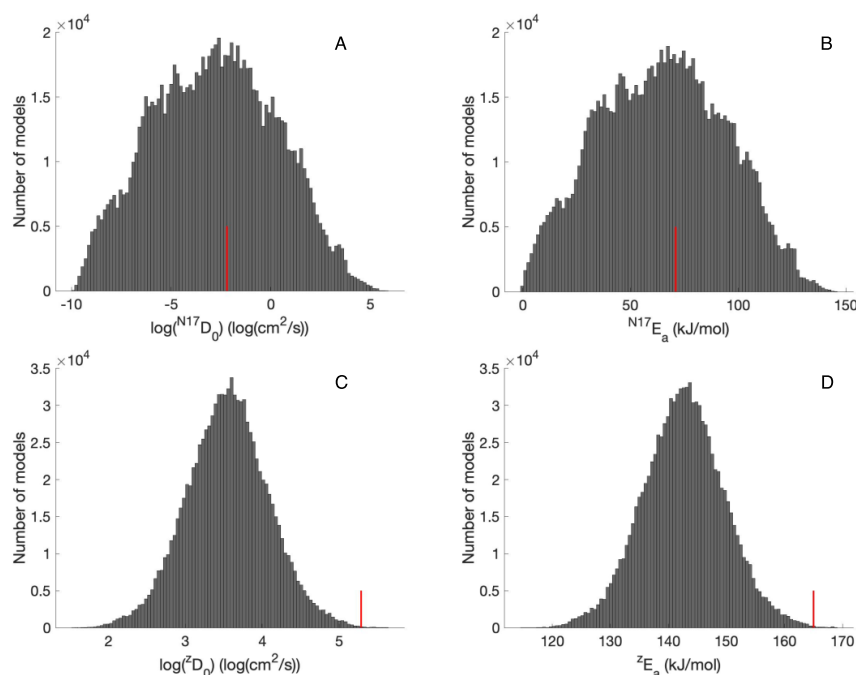


**Figure 2.** The sampled marginal posterior distributions for the four diffusion parameters representing the two hypothetical crystals. A) and B) are the frequency factor ( $^{17}D_0$ ) and activation energy ( $^{17}E_a$ ), respectively, for a damaged, amorphous crystal. C) and D) are the frequency factor ( $^2D_0$ ) and activation energy ( $^2E_a$ ), respectively, for an undamaged crystal. The red lines show the values of these parameters used by Guenther et al., (2013).

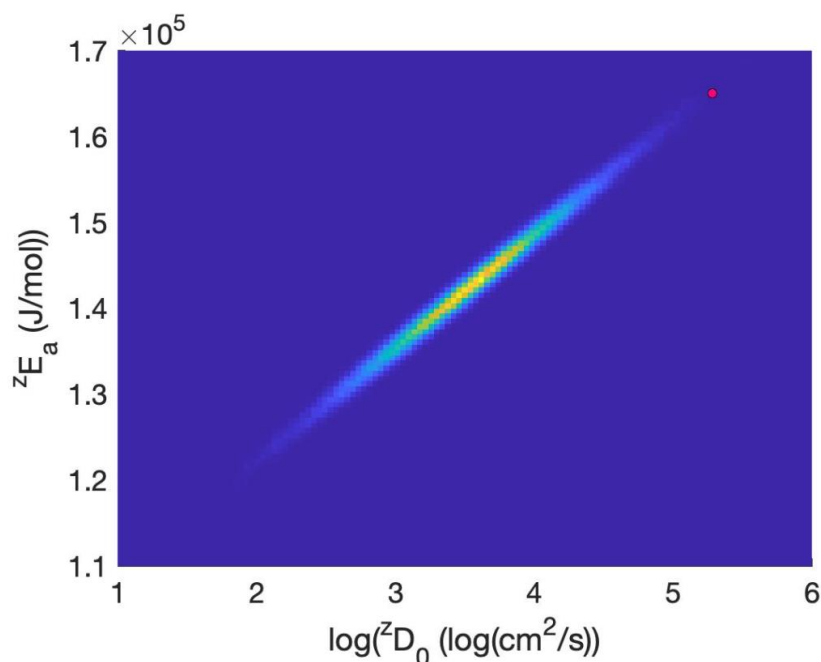


Figure 3. Inferred model parameters from diffusion data are strongly correlated. Our approach to infer the diffusion kinetics of the hypothetical crystals using the radiation damage model maintains this correlation.

425 This is clearly illustrated with the diffusion parameters for the undamaged crystal. The pink spot shows the diffusion kinetics inferred by Guenther et al., (2013) and shows that it is reasonably far from the center of our distribution, but still falls on the clear correlation trend we define. The colours are proportional to posterior probability with oranges reflecting highest probability.



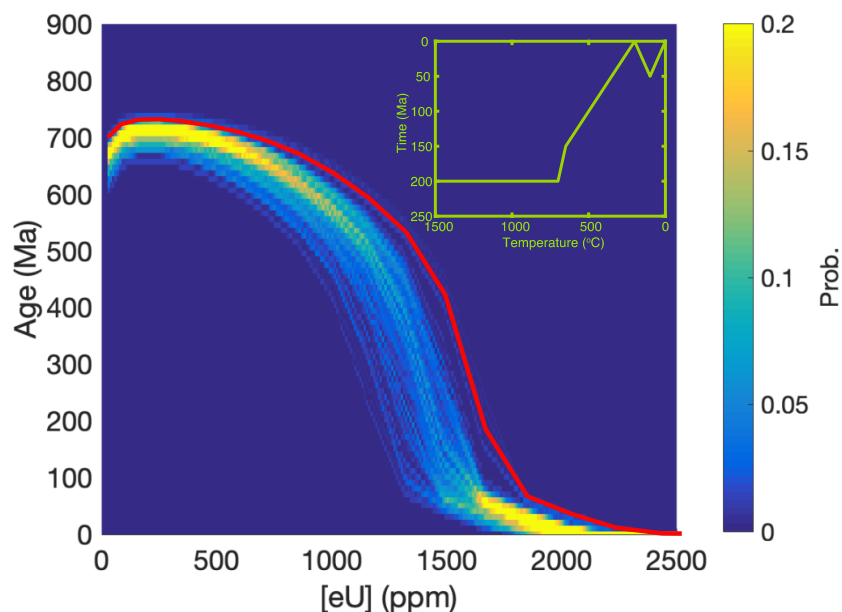
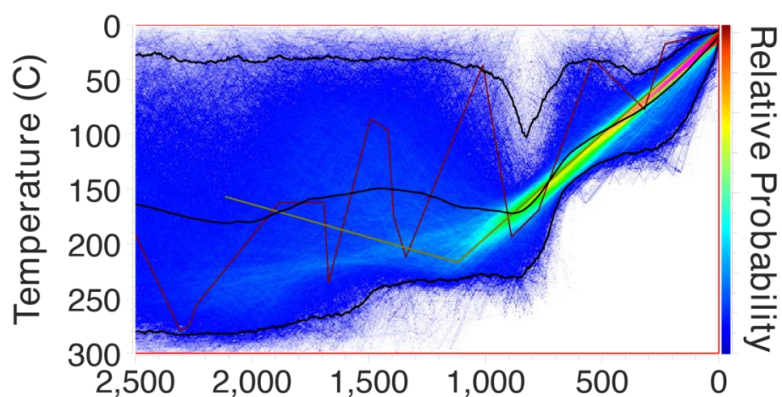


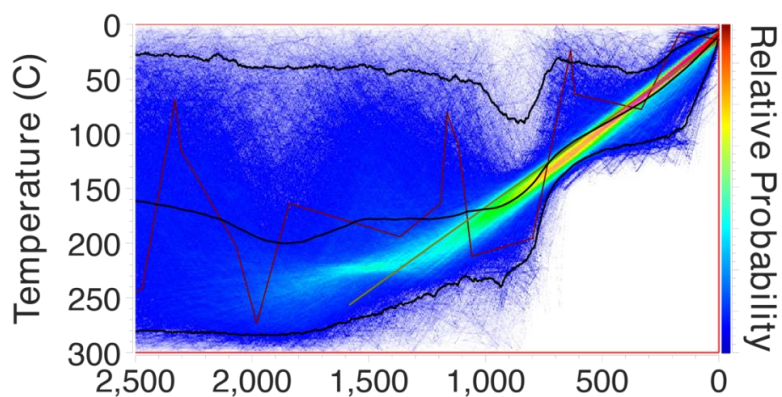
Figure 4. Propagating uncertainties in the radiation damage model produces a wide range of ZHe ages for a specific amount of damage. The red line shows the predicted age-[eU] relationship using the canonical values of the radiation damage and annealing model. The continuous thermal history used to produce the result is shown in the inset.



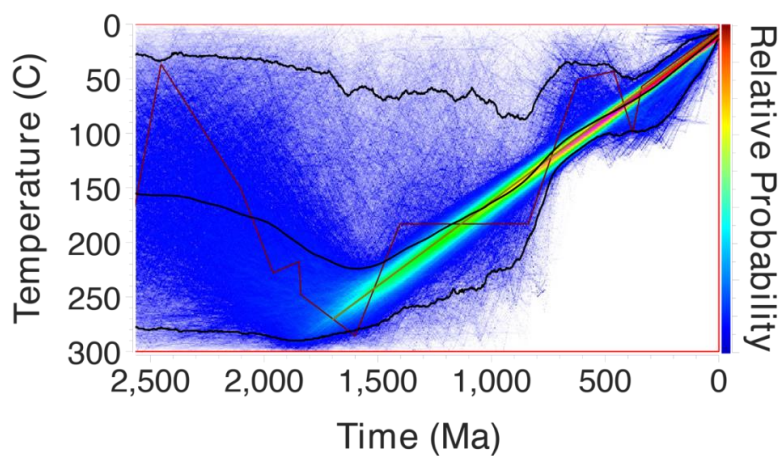
### A) ZRDAAM Model Parameters



### B) High amorphous frequency factor



### C) Low amorphous frequency factor





450 **Figure 5. Different parameter values for the damage model lead to differences in inferred thermal histories.**  
 A) The thermal history recovered from QTQt using the canonical values of the radiation damage model  
 from Guenther et al., (2013). The colours are proportional to posterior probability, the grey line is the  
 maximum a posteriori model and the stepped line is the maximum likelihood model. The three curved lines  
 are the expected model with the upper and lower credible intervals, please refer to Gallagher (2012) for  
 455 more details on QTQt. B) and C) The recovered thermal histories using different parameter sets with a high  
 value and a low value of the amorphous frequency factor, respectively. The values for the two parameter  
 sets are 129224.284308, 4.000427, 149756.087043, 4.130064 and 42388.297312, -5.000653 137904.535009,  
 3.253373 for  $NI7_{Ea}$ ,  $\log_{10}(NI7_{D0})$ ,  $ZEa$ , and  $\log_{10}(Z_{D0})$ . These exact values are drawn from the Markov  
 Chain in order to ensure that they account for the complex model correlations. The overall patterns are  
 460 very similar, but the apparent resolution is different, resulting in different geological conclusions.

465

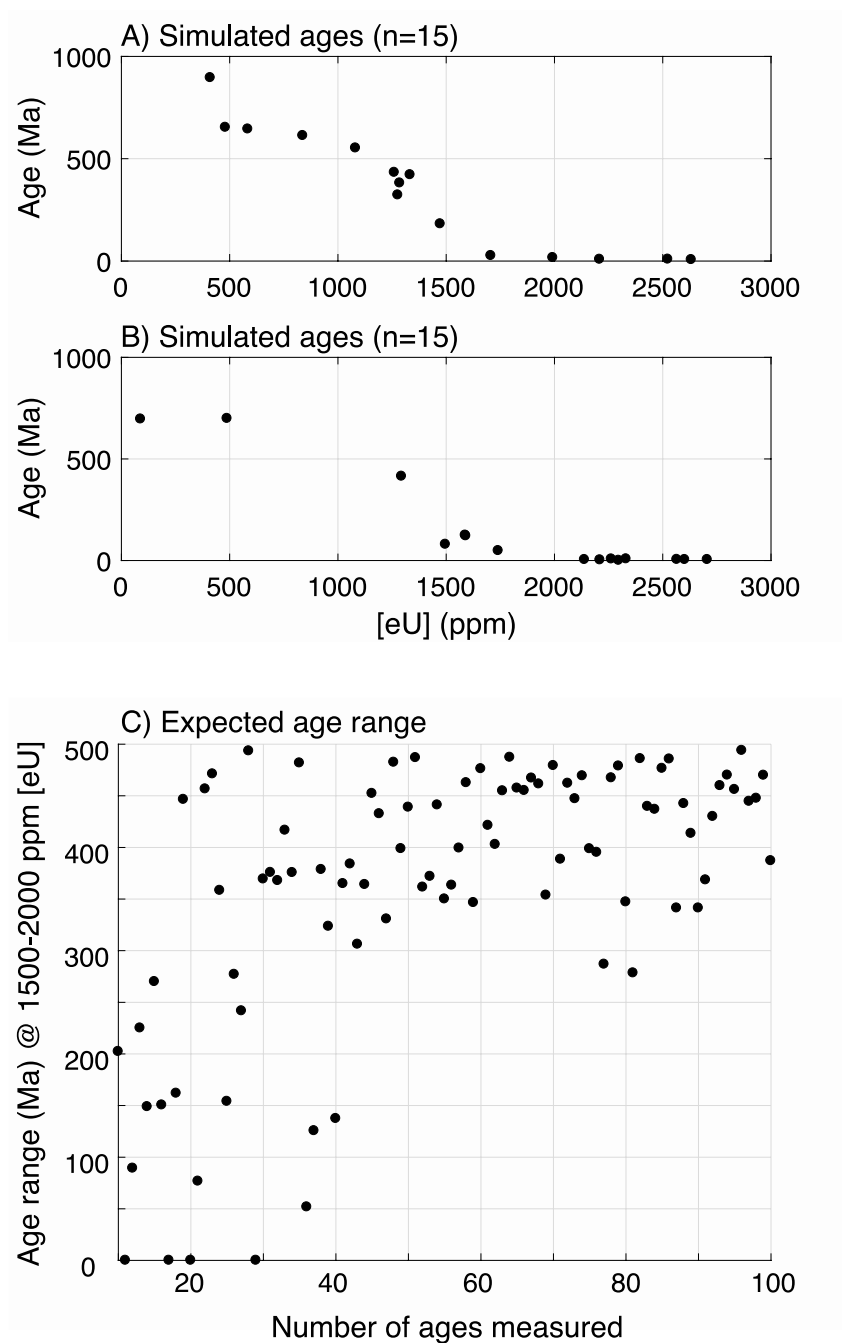


**Figure 6.** Model realizations and expected ranges of ages. A & B) random samples are drawn from the probability distribution in Figure 4 to highlight the sorts of datasets that are expected given the typical number of ages measured on a single sample. The simulated ages are different between the two realizations



470 of a typical dataset. C) Many ages need to be sampled in order to accurately capture the spread in ages over  
a specific [eU] bin. It is challenging to measure the spread because there is no easy way to estimate the  
amount of radiation damage a crystal has accumulated until after the helium concentration has been  
measured.

475

480

485